

Effect of Substrate and Process Parameters on the Gas-Substrate Convective Heat Transfer Coefficient During Cold Spraying

Amirhossein Mahdavi¹ · André McDonald¹

Submitted: 18 May 2017 / in revised form: 30 October 2017 / Published online: 13 November 2017
© ASM International 2017

Abstract The final quality of cold-sprayed coatings can be significantly influenced by gas-substrate heat exchange, due to the dependence of the deposition efficiency of the particles on the substrate temperature distribution. In this study, the effect of the air temperature and pressure, as process parameters, and surface roughness and thickness, as substrate parameters, on the convective heat transfer coefficient of the impinging air jet was investigated. A low-pressure cold spraying unit was used to generate a compressed air jet that impinged on a flat substrate. A comprehensive mathematical model was developed and coupled with experimental data to estimate the heat transfer coefficient and the surface temperature of the substrate. The effect of the air total temperature and pressure on the heat transfer coefficient was studied. It was found that increasing the total pressure would increase the Nusselt number of the impinging air jet, while total temperature of the air jet had negligible effect on the Nusselt number. It was further found that increasing the roughness of the substrate enhanced the heat exchange between the impinging air jet and the substrate. As a result, higher surface temperatures on the rough substrate were measured. The study of the effect of the substrate thickness on the heat transfer coefficient showed that the Nusselt number that was predicted by the model was independent of the thickness of the substrate. The surface temperature profile, however, decreased in increasing radial distances from the stagnation point of the impinging jet as the thickness of the

substrate increased. The results of the current study were aimed to inform on the influence and effect of substrate and process parameters on the gas-substrate heat exchange and the surface temperature of the substrate on the final quality of cold-sprayed coatings.

Keywords cold spraying · convective heat transfer coefficient · jet impingement · process parameters · substrate roughness · surface temperature

List of symbols

A	Surface area
b	Radius of the substrate (m)
c	Speed of sound (m/s)
C_p	Specific heat capacity (J/K)
C_f	Skin friction coefficient
D	Cold spray nozzle diameter
h	Heat transfer coefficient (W/m ² -K)
I	Intensity of emitted radiation (W/sr-Hz)
J	Bessel function
k	Thermal conductivity (W/m-K)
N	Norm of the differential equation
P	Total pressure (Pa)
\dot{Q}	Heat transfer rate
r	Radial coordinate
R	Surface roughness
\bar{R}	Gas constant (J/kg-K)
r'	Radial dummy variable (m)
t	Time (s)
T	Temperature/total temperature (°C)
T_0	Substrate initial temperature (°C)
u'	Fluctuating component of velocity
\bar{u}	Mean velocity
V	Velocity (m/s)

✉ Amirhossein Mahdavi
amahdavi@ualberta.ca

¹ Department of Mechanical Engineering, University of Alberta, 10-203 Donadeo Innovation Center for Engineering, Edmonton, AB T6G 1H9, Canada

\bar{V}	Average velocity (m/s)
z	Axial coordinate
Z	Compressibility factor
z'	Axial dummy variable (m)

Non-dimensional parameters

Fo	Fourier number, $Fo = \frac{\alpha_i t}{\delta^2}$
Ma	Mach number, $Ma = \frac{V_a}{c}$
Nu	Nusselt number, $Nu = \frac{hD_n}{k_g}$
Re	Reynolds number, $Re = \frac{\rho_a V_a D_n}{\mu_a}$

Greek symbols

α	Thermal diffusivity (m ² /s)
β	Eigenvalues in axial coordinate
δ	Thickness of the substrate (m)
ε	Emissivity
ζ	Eigenvalues in radial coordinate
η	Non-dimensional radius
θ	Non-dimensional temperature
λ	Wavelength (μm)
μ	Dynamic viscosity (kg/m-s)
ρ	Density (kg/m ³)
τ	Shear stress (N/m ²)

Subscripts

a	Air
ave	Average
AW	Adiabatic wall
b	Black body
e	Real surface
g	Propellant gas
i	Numerator in radial coordinate
j	Numerator in axial coordinate
ku	Kurtosis
m	Mean
n	Nozzle
s	Substrate/surface
sk	Skewness
ss	Steady-state
w	Wall
∞	Ambient

Introduction

Cold-gas dynamic spraying is a coating fabrication process in which a supersonic gas flow is produced and used to propel un-melted metal or alloy powder particles to deposit, with high impact forces, upon a substrate to form a highly adherent coating (Ref 1). Due to the high velocity of the under-expanding gas jet upon the substrate (Ref 2), and the high temperature of the impinging jet, a significant

amount of thermal energy is expected to be transferred from the gas jet to the substrate (Ref 3, 4). The high velocity of the impinging gas on the flat substrate, furthermore, ensures that the predominant mode of heat transfer is convection. Therefore, determining the convective heat transfer coefficient will enable the determination of the heat transfer rate from the impinging gas jet to the substrate, or previous layers of the deposited coating. Process parameters, such as the temperature and the pressure of the propellant gas, and substrate parameters, such as the substrate roughness and thickness, can also affect the heat transfer rate from the gas jet to the substrate. It has been further shown that the final quality of cold-sprayed coatings is noticeably influenced by gas-substrate heat exchange due to the dependence of the adhesion strength of the particles on the substrate temperature (Ref 5), i.e., the adhesion strength of cold-sprayed particles can be increased by heating the substrate. For instance, Watanabe et al. (Ref 5) showed that the adhesion strength of Al coatings on the aluminum alloy (A5083) substrate at 200 °C was approximately 2.5 and 5.5 times higher than that with temperatures of 100 and 25 °C, respectively. Therefore, studying the effects of the cold spray parameters on the heat exchange and surface temperature of the substrate and the coating becomes important.

It has been shown that higher gas pressure causes an increase in gas density, resulting in increased acceleration of the particles (Ref 6). Moreover, an alternative to increasing the speed of the gas and the particles is to pre-heat the propellant gas (Ref 6, 7). In this regard, several studies have been conducted to investigate the effect of the gas temperature and pressure on the particle velocity and the deposition efficiency of the cold-sprayed coatings (Ref 8-11). For instance, Legoux et al. (Ref 8) showed that the particle velocity of the Al and Zn particles, as well as the deposition efficiency of the cold-sprayed Al and Zn coatings increased significantly, as the gas temperature increased. In a parallel study, Fukumoto et al. (Ref 9) argued that the higher substrate temperature resulted in a higher deposition efficiency of Cu particles, when the particles were held at room temperature. They concluded that although higher velocity and temperature of the gas and the deposited particles are influential parameters for higher deposition efficiency of cold-sprayed particles and coatings, higher surface temperature of the substrate may result in a similar outcome vis-à-vis the deposition efficiency (Ref 9). It can be inferred from the aforementioned studies that the heat transfer rate between the gas and the substrate, which would in turn affect the substrate temperature, may affect the deposition efficiency of the cold-sprayed coatings. Therefore, in addition to these studies, the study of the effect of the gas temperature and pressure on the convective heat transfer coefficient and heat

exchange between the under-expanded gas and the substrate is required.

In addition to the major effect of the process parameters, the surface roughness of the substrate may also influence the substrate temperature distribution and heat transfer rate between the substrate and the impinging cold spray air jet. This is due to the topological changes on the substrate surface to which heat transfer occurs. In this regard, the effect of patterns on fabricated surfaces on the heat transfer coefficient of an impinging air jet on those types of surfaces has been studied (Ref 12–14). Chakroun et al. (Ref 12) patterned a surface with cubes of 1 mm length, which were distributed uniformly along the substrate to simulate a rough surface. It was shown that the local and average Nusselt number of the impinging air jet on the fabricated rough surface with Reynolds number ranging from 6500 to 19,000 increased from 8.9 to 28% compared to that on the smooth surface (Ref 12). In a similar study, Beitelmal et al. (Ref 13) employed a circular array of protrusions of 0.5 mm base diameter and 0.5 mm high. The results of their study indicated that the Nusselt number over the rough surface increased up to 6% for an impinging air jet with Reynolds number ranging from 9600 to 38,500. In a recent numerical study, Dobberteau and Rahman (Ref 14) calculated the Nusselt number for an impinging air jet with Reynolds number of 500 to 1000 over a rough surface consisting of indentation depths ranging from 0.125 to 0.5 mm. While these studies have placed emphasis on substrates with patterned surfaces, an investigation of the effect of the surface roughness generated by grit-blasting on the heat transfer coefficient of the impinging air jet, within the domain of application of cold spraying, is still lacking.

The effect of the substrate thickness on the heat transfer coefficient and the surface temperature of the substrate was cursorily studied. In a numerical study by McDonald et al. (Ref 15), the effect of substrate thickness on the maximum surface temperature of the substrate of different materials was explored. It was shown that for all the materials that were studied, the maximum surface temperature decreased as the thickness of the substrate increased (Ref 15). A complementary study with emphasis on the effect of the substrate thickness on the gas-substrate convective heat transfer coefficient can serve to expand on the findings of previous investigations.

In the present work, through a semi-empirical analytical study, the effect of process parameters, such as air (working gas) temperature and pressure, and substrate parameters, including surface roughness and thickness, on the heat transfer coefficient and surface temperature during the cold spray process was investigated. The purpose of this study was to highlight the parameters that influence the heat exchange from the impinging air jet on the flat

substrate, which eventually affects the final quality of the cold-sprayed coating.

Experimental Method

Cold Spray Deposition System

A low-pressure cold-gas dynamic spraying unit (SST Series P, Centerline, Ltd., Windsor, ON, Canada) was utilized to produce a supersonic air jet. The nozzle of the cold spray unit was a 140-mm-long converging–diverging de Laval nozzle, with throat and exit diameters of 2.54 mm and 6.3 mm, respectively. The system parameters of the low-pressure cold spray unit that were used in this study are summarized in Table 1. The cold spray nozzle was directed at the center of the front surface of the substrate and was held stationary at the specified stand-off distance.

Substrate Preparation

In this study, aluminum 6061-T6 was used as the substrate. This material is known to have relatively high thermal conductivity (order of 160 W/m-K), which increases heat conduction through the substrate. Thus, this material is expected to achieve steady-state thermal conditions quickly after impingement of the hot air jet on the substrate. It should be mentioned that this material was chosen to expedite the experimentation process; however, other materials can be considered as the substrate on which to conduct the experiments. The geometry of the substrate was a disk with dimension of 200 mm in diameter. The thickness of the substrate was 1.5, 2.5, or 6.5 mm. In order to prevent the back surface of the substrate from exchanging heat with the ambient air, a thermal insulation material, vitreous aluminosilicate fiber (ISAFORM 2300° L.O., Insulation Specialties of America, Inc., Watah, IN, USA), was attached at the back surface of the substrate. The substrate was mounted onto a substrate holder. Figure 1 shows a photograph and a schematic of the experimental assembly.

In order to study the effect of the substrate roughness on the heat transfer coefficient and surface temperature of the substrate, the cold spray unit was used to grit-blast the 2.5-mm-thick aluminum substrate by depositing garnet sand

Table 1 Low-pressure cold spray system parameters

Pressure range	660–830 kPa (96–120 psig)
Temperature range	100–300 °C
Stand-off distance (SOD)	25 mm

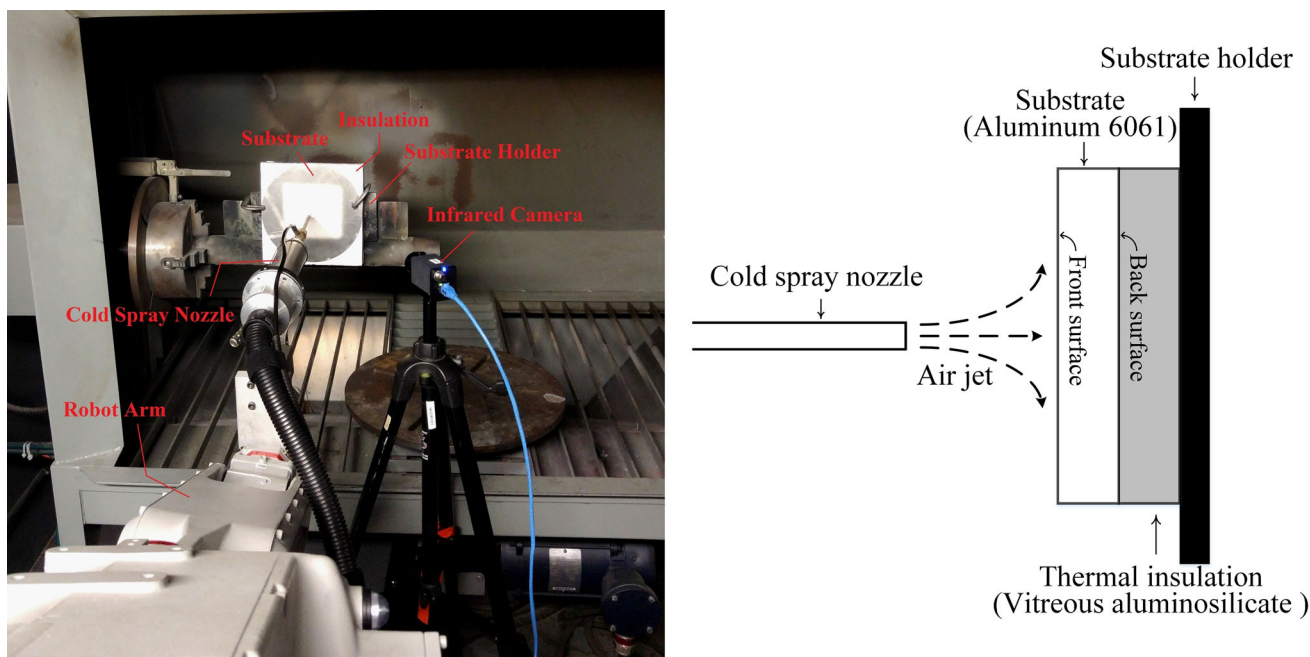


Fig. 1 Actual image and schematic of the experimental assembly

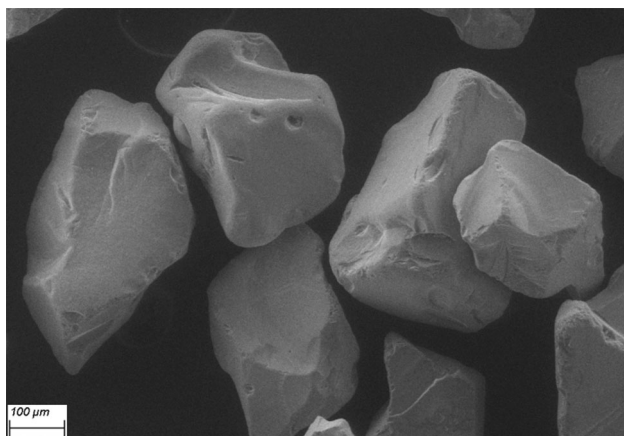


Fig. 2 Morphology of the garnet sand particles

particles (Super Garnet, V.V. Mineral, Tamil Nadu, India). The morphology of the garnet sand particles was examined by using a scanning electron microscope (EVO MA 12, Zeiss, Cambridge, UK) that was set in the secondary electron mode. Figure 2 shows the morphology of the garnet sand particles. By using the image analysis software (ImagePro, Media Cybernetics, Bethesda, MD, USA), the average diameter of the garnet sand particles was measured to be $340 \pm 54 \mu\text{m}$ ($n = 5$), where n represents the number of particles. A confocal scanning microscope (Axio CSM 700, Carl Zeiss MicroImaging GmbH, Jena, Germany) was employed to study the topology and the roughness parameters of the grit-blasted substrate.

Temperature Measurement

The transient and steady-state temperatures of the front surface of the substrate were measured by using a calibrated infrared camera (FLIR A65, FLIR Systems, Inc., Nashua, NH, USA). The spatial resolution or Instantaneous Field of View (IFOV) of the camera was 1.31 mrad. The infrared camera had a spectral range of 7.5 to 13 μm and a time resolution of 12 ms. The image capture frequency of the camera was 9 Hz, and the measurement accuracy was $\pm 5 \text{ }^\circ\text{C}$ or 5% of the reading. In the case of smooth (polished) substrates, to enable more accurate measurements, the front surface of the substrate was painted black so as to approach conditions of a black body. Accordingly, the emissivity of the substrate was set to 0.96 on the infrared camera. However, for the grit-blasted (roughened) substrate, it was not reasonable to paint the front surface, since the black paint would fill the asperities of the substrate and cause rough surface to become smooth. Therefore, in order to measure the surface temperature of the roughened surface by using the infrared camera, the emissivity of the rough substrate was first evaluated. To this end, an experiment was conducted to measure the temperature-dependent emissivity of the rough aluminum substrate. A substrate holder was fabricated from copper, where two cartridge heaters (50 W Miniature High Temperature Cartridge Heater (D1/8" \times 1 1/4"), McMaster-Carr, Aurora, OH, USA) were embedded inside the copper holder. A temperature controller (CNI8A42, Omega Engineering Inc., Stamford, CT, USA) that was equipped

with a J-type thermocouple was employed to adjust the temperature of the substrate holder to the desired set-point (Ref 16). The setup was used to heat up the rough substrate. The surface temperature of the substrate was measured by using an external J-type thermocouple. Simultaneously, the infrared camera was directed at the substrate. The emissivity that was indicated on the infrared camera was modified until the temperature measurement on the infrared camera read-out panel was in accord with the measurement of the thermocouple. Figure 3 shows a schematic of the experimental assembly that was used to measure the emissivity of the rough substrate.

Mathematical Model

A significant amount of thermal energy is expected to be transferred between the air jet from the cold spray nozzle and the substrate due to the impingement of the supersonic hot air jet on the flat substrate. The predominant mode of heat transfer between the impinging air jet and the substrate is forced convection; therefore, estimates of the convective heat transfer coefficient (h) are required in order to determine the heat flux and the temperature distribution within the substrate. A detailed semi-empirical analytical heat transfer model to evaluate the radial convective heat transfer coefficient between a flat substrate and an under-expanding supersonic air jet generated by a cold spray system has been developed elsewhere (Ref 17, 18). The model by Mahdavi and McDonald (Ref 17) is further capable of estimating the transient temperature distribution within the substrate during the impingement of the air jet. Since analytical determination of the heat transfer coefficient is outside the scope of the current study and it has been developed elsewhere, a summary of the heat transfer coefficient model is described here. A schematic of the geometry of the model problem is shown in Fig. 4. There was heat flux on the exposed front surface of the substrate due to the impingement of the air

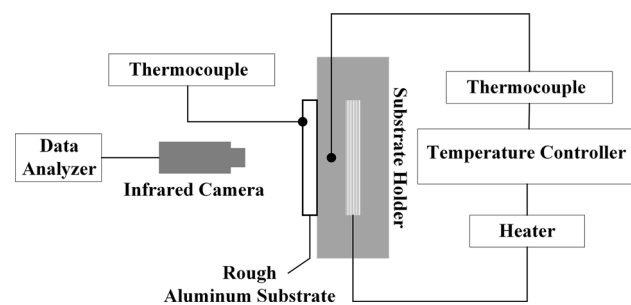


Fig. 3 Schematic of the experimental assembly for measuring the emissivity of rough aluminum substrate (Ref 16)

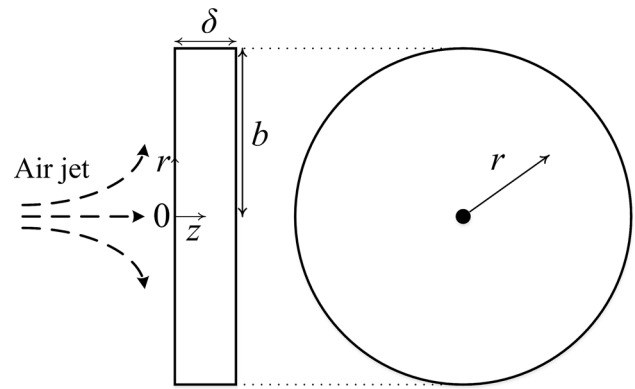


Fig. 4 Schematic of the geometry for the mathematical model (Ref 17)

jet, while all other sides of the substrate were assumed to be insulated. The thickness of the substrate (δ) was much smaller than its radius (b); therefore, the surface area of the collateral side from which heat was likely lost was assumed to be negligible in comparison with the heat gain on the front surface of the substrate.

The governing equation of the transient two-dimensional heat conduction model within the substrate is

$$\frac{1}{r} \frac{\partial}{\partial r} \left(r \frac{\partial T}{\partial r} \right) + \frac{\partial^2 T}{\partial z^2} = \frac{1}{\alpha_s} \frac{\partial T}{\partial t} \tag{Eq 1}$$

The boundary conditions and the initial condition are

$$T(r = 0, z, t) = \text{finite}, \tag{Eq 2}$$

$$\frac{\partial T(r = b, z, t)}{\partial r} = 0, \tag{Eq 3}$$

$$-k_s \left[\frac{\partial T(r, z = 0, t)}{\partial z} \right] = h(r) [T_{AW}(r) - T(r, z = 0, t)], \tag{Eq 4}$$

$$\frac{\partial T(r, z = \delta, t)}{\partial z} = 0, \tag{Eq 5}$$

$$T(r, z, t = 0) = T_0. \tag{Eq 6}$$

In Eq 4, h is the convective heat transfer coefficient between the substrate and the impinging air jet and T_{AW} represents the adiabatic wall temperature. A Green's function approach was employed to solve the governing equation of this problem. A detailed description of the calculation methodology that involves use of the Green's function and the formulation of the model are provided by the authors elsewhere (Ref 17). The final expression for the temperature distribution within the substrate was found to be

$$\begin{aligned}
T(r, z, t) = & \sum_{i=1}^{\infty} \sum_{j=1}^{\infty} \left[T_0 \frac{\exp[-\alpha_s(\zeta_i^2 + \beta_j^2)t]}{N(\zeta_i)N(\beta_j)} \right. \\
& \times J_0(\zeta_i r) [\tan(\beta_j \delta) \sin(\beta_j z) + \cos(\beta_j z)] \\
& \times \int_{r'=0}^b \int_{z'=0}^{\delta} J_0(\zeta_i r') [\tan(\beta_j \delta) \sin(\beta_j z') + \cos(\beta_j z')] r' dz' dr' \\
& + \left(\frac{\alpha_s}{k_s} \right) \left[\frac{h(r)}{N(\zeta_i)N(\beta_j)} \right] J_0(\zeta_i r) [\tan(\beta_j \delta) \sin(\beta_j z) + \cos(\beta_j z)] \\
& \times \frac{1}{\alpha_s(\zeta_i^2 + \beta_j^2)} [1 - \exp(-\alpha_s(\zeta_i^2 + \beta_j^2)t)] \\
& \times \left. \int_{r'=0}^b J_0(\zeta_i r') T_{AW}(r') r' dr' \right], \quad (\text{Eq 7})
\end{aligned}$$

where ζ_i and β_j are the eigenvalues in the radial ($0 \leq r \leq b$) and the axial ($0 \leq z \leq \delta$) coordinates, respectively, and they can be obtained from

$$\zeta_i J_1(\zeta_i b) = 0, \quad \text{and} \quad (\text{Eq 8})$$

$$\beta_j \tan(\beta_j \delta) - \frac{h(r)}{k_s} = 0. \quad (\text{Eq 9})$$

In Eq 7, $N(\zeta_i)$ and $N(\beta_j)$ are the Norms of the differential equations in the radial and axial coordinates, respectively, and they are

$$N(\zeta_i) = \int_{r=0}^b J_0^2(\zeta_i r) r dr, \quad \text{and} \quad (\text{Eq 10})$$

$$N(\beta_j) = \int_{z=0}^{\delta} [\tan(\beta_j \delta) \sin(\beta_j z) + \cos(\beta_j z)]^2 dz. \quad (\text{Eq 11})$$

Analytical determination of the transient temperature distribution within the flat substrate that was exposed to an under-expanding supersonic air jet of a cold spray system is given by Eq 7. Equation 7 and 9 can be used to determine the value of the heat transfer coefficient under various substrate conditions. The shooting method was applied to estimate the spatial distribution of the heat transfer coefficient across the substrate surface under the impinging and spreading air jet. A zero-dimensional code that was developed in MATLAB (MathWorks, Inc., Natick, MA, USA) was used to solve the explicit expression for $h(r)$ by using Eq 7, 8, and 9. Terms in the infinite series of Eq 7 were added until the solutions converged to within 2% of the sum.

Results and Discussion

Effect of Process Parameters on the Heat Transfer Coefficient

The radial variation of the convective heat transfer coefficient between the flat substrate and the impinging under-expanding supersonic air jet was estimated under various combinations of the air total pressure and total temperature of the gas jet. By definition, the total pressure represents the pressure of the air when it is adiabatically brought to rest, and it refers to the pressure of the air before it enters the converging–diverging nozzle. Similarly, the total temperature is defined as the air temperature before it enters the nozzle (Ref 19). The thickness of the substrate was 1.5 mm. It has been shown that the heat transfer coefficient of the under-expanding air jet is time-independent (Ref 17). In other words, the time that the nozzle remained stationary over the substrate would not affect the convective heat transfer coefficient of the impinging air jet. However, the temperature difference between the air film and the substrate can be affected by the duration of the impingement of the air jet over the substrate. The heat transfer coefficient is heavily dependent on the velocity of the under-expanding air jet, and since the velocity of the impinging jet is almost constant, the heat transfer coefficient would likely remain unchanged during the impingement of the air jet. Therefore, the heat transfer coefficient was estimated at an arbitrary time after the nozzle had been held stationary over the substrate. It is common to express the time as the non-dimensional Fourier number, defined as

$$Fo = \frac{\alpha_s t}{\delta^2}. \quad (\text{Eq 12})$$

For most of the scenarios that were explored in this paper, the heat transfer coefficient was estimated at $Fo = 81$. This value of Fo was calculated after 3 s of the nozzle remaining stationary over the substrate to ensure that the measurements of the surface temperature profile were taken before reaching the steady-state condition in order to take into account the effect of time. The reason for measuring the surface temperature before reaching steady-state condition was to validate the capability of the model to determine the surface temperature of the substrate at any desired time after impingement of the cold spray air jet. In this study, the heat transfer coefficient was presented in the form of the non-dimensional Nusselt number, which is defined as

$$Nu = \frac{h D_n}{k_g}. \quad (\text{Eq 13})$$

The effect of the total pressure of the air jet on the Nusselt number of the impinging and spreading air jet was investigated. The total temperature of the air was set to

200 °C on the cold spray unit console. Figure 5 shows the Nusselt number as a function of the non-dimensional radial distance from the stagnation point of the jet on the substrate at total pressures of the air of 660, 745, and 825 kPa. The radial distance from the stagnation point was non-dimensionalized with respect to the nozzle diameter as

$$\eta = \frac{r}{D_n} \tag{Eq 14}$$

Figure 5 shows that the Nusselt number of the impinging air jet on the substrate increased as the total pressure of the air jet increased. This is likely related to the notable effect of the air pressure on the density of the air, which was the working fluid in this study. According to the equation of state of a real gas at constant temperature, the density of the air will increase with increasing air pressure. The equation of state of a real gas is (Ref 20)

$$P = Z\rho\bar{R}T, \tag{Eq 15}$$

where Z is the compressibility factor of the working gas. As a result of the increase in the density of the air, the momentum of the air jet increases. Given that the momentum of the gas will likely decrease as the jet impacts and spreads on the surface, the change in momentum will manifest itself as an increase in inertial force. Thus, the Reynolds number of the air jet will increase. By definition, the Reynolds number is the non-dimensional ratio of the inertial force and the viscous force within the fluid, and for an impinging jet it is expressed as

$$Re = \frac{\rho_a V_a D_n}{\mu_a} \tag{Eq 16}$$

It has been reported that the Nusselt number for both laminar and turbulent compressible flow is directly proportional to approximately the square root of the Reynolds number of the fluid (Ref 21). In light of the proportional

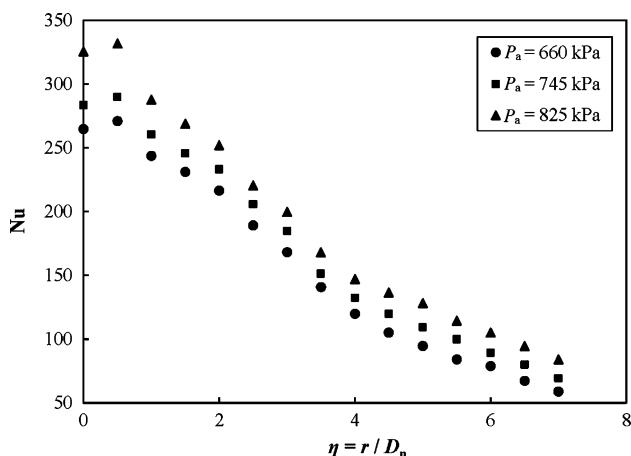


Fig. 5 Radial variation of the Nusselt number of the under-expanding air jet over the substrate for different total pressures of the air jet

relationship between the air pressure, air density, the Reynolds number, and the Nusselt number, it can be deduced that the increase in the gas pressure would increase the Nusselt number between the substrate and the impinging air jet. Other air properties that affect the Nusselt number, such as thermal conductivity, dynamic viscosity, and Prandtl number are not noticeably dependent on the air pressures that are utilized during cold spraying (Ref 22).

The effect of the total temperature of the air on the Nusselt number of the impinging air jet was investigated. The total pressure of the air was set to 660 kPa on the cold spray unit console. Figure 6 presents the radial variation of the non-dimensional Nusselt number for three different air temperatures of 100, 200, and 300 °C. The estimated profiles for the Nusselt number in Fig. 6 nearly coalesced for all air temperatures. Increasing the total temperature of the air decreased the density and increased the dynamic viscosity of the air (Ref 20), which directly corresponds to lower inertial force and higher viscous force of the impinging air jet. Therefore, it is expected that the Reynolds number of the impinging air jet, and as a result, the Nusselt number of the impinging air jet, decreased. But, along with the two aforementioned outcomes, increasing the total temperature of the air will increase the velocity of the air jet. In order to have supersonic air flow at the converging–diverging nozzle exit, the Mach number of the air at the location of the nozzle throat must be unity ($Ma = \frac{V_a}{c} = 1$) (Ref 19). Since the speed of sound increases with an increase in the air temperature (Ref 20), the velocity of the air must increase in order that the Mach number at the nozzle throat remains constant at unity. The velocity of the air at the nozzle throat for a supersonic air jet is formulated as

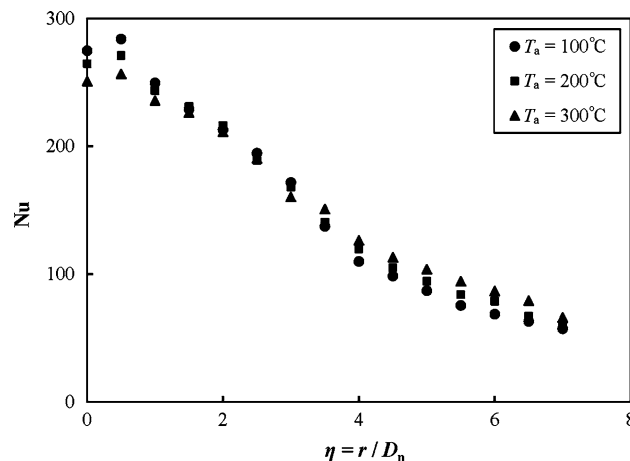


Fig. 6 Nusselt number of the under-expanding air jet over the substrate vs. non-dimensional radius for different total temperatures of air

$$V_a = \sqrt{\gamma \overline{RT_a}} \quad (\text{Eq 17})$$

It is expected that the increase in air velocity, as a result of the increase in the air temperature, would neutralize the effects of the reduction in inertial force, which was due to the decrease in the air density. Therefore, the Reynolds number of the air jet would not change significantly by increasing the total temperature of the air. Accordingly, the radial variation of the Nusselt number of the under-expanding air jets nearly coalesced as observed in Fig. 6.

Although the Nusselt number of the impinging air jet is independent of the total temperature of the air, this does not suggest that the heat transfer coefficient between the substrate and the impinging air jet is independent of the total temperature of the air. It is hypothesized that the dependence of the thermal conductivity of the air on its temperature would compensate for the changes in the heat transfer coefficient of the impinging air jet as a result of increasing the total temperature of the air. Therefore, the heat transfer coefficient at total temperatures of air of 100, 200, and 300 °C for different radial distances from the stagnation point of the jet on the substrate was determined, as shown in Fig. 7. The results show that the heat transfer coefficient between the substrate and the impinging air jet increased slightly, as the total temperature of the air increased. This was due to the strong dependency of the forced convective heat transfer coefficient on the velocity of the air (Ref 21). Taking into account Fig. 6 and 7, it can be inferred that studying the heat transfer coefficient may be more effective in investigating the heat exchange between the substrate and the impinging air, especially when the thermo-physical properties of the working gas are highly dependent on process parameters such as temperature.

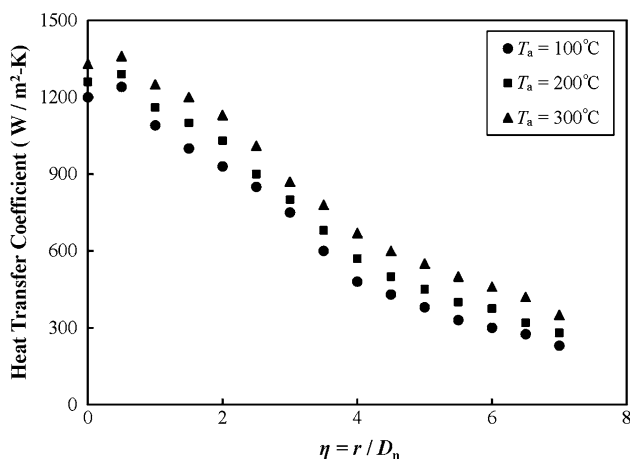


Fig. 7 Heat transfer coefficient of the under-expanding air jet over the substrate vs. the non-dimensional radius for different total temperatures of air

Effect of Substrate Parameters on Heat Transfer Coefficient

Effect of Surface Roughness on Heat Transfer Coefficient and Surface Temperature

In order to improve the mechanical interlock between the substrate and the deposited coating during cold spraying, the substrate is conventionally roughened by employing a surface preparation technique such as grit-blasting or shot peening. These techniques are also used to decrease or remove the oxide layer that inherently grows on metal substrate surfaces to allow for further improvement of the adhesion of the coating on the substrate (Ref 23). Increasing the roughness of the substrate may also affect the heat exchange between the substrate and the impinging air jet of the cold spray system, since it changes the surface topology from which the heat transfer occurs. Therefore, the effect of the surface roughness on the surface temperature profile of the substrate and the convective heat transfer coefficient between the substrate and the impinging air jet was investigated. To that end, the cold spray unit was utilized to blast garnet sand particles onto the aluminum 6061-T6 substrate to roughen the surface. A confocal microscope was used to study and evaluate the topology and roughness parameters of the smooth and roughened substrates within a surface scan area of $1150 \times 1150 \mu\text{m}^2$ from the front surface of the substrate.

Figure 8 compares the surface topologies and the peaks and valleys of the asperities of the smooth and the roughened (grit-blasted) substrates. The contour bar on the left hand side of Fig. 8 shows the magnitude of the asperities on the smooth and rough substrates. The maximum values of the contour bars are different for the images. As shown in the figure, the magnitude of the peaks and valleys of the asperities on the rough (grit-blasted) surface is significantly higher than that on the smooth substrate. Three roughness parameters of the substrate, namely average roughness (R_{ave}), skewness (R_{sk}), and kurtosis (R_{ku}) (Ref 24), were investigated in order to provide a better understanding of the results shown in Fig. 8. By definition, the average roughness (R_{ave}) is the average of the distance of the asperities from a hypothetical mean plane. Skewness (R_{sk}) is defined to show the symmetry of the peaks and valleys of the asperities with regard to the hypothetical flat plane. Surfaces with positive R_{sk} have relatively high peaks, while surfaces with negative R_{sk} have deep valleys and fairly smoother plateaus (Ref 25). Kurtosis (R_{ku}) represents the degree of pointedness of the asperities on the front surface. Surfaces with higher values of R_{ku} exhibit steep asperities; as the R_{ku} becomes smaller, the surface becomes smoother (Ref 25). Table 2 shows the values of the aforementioned

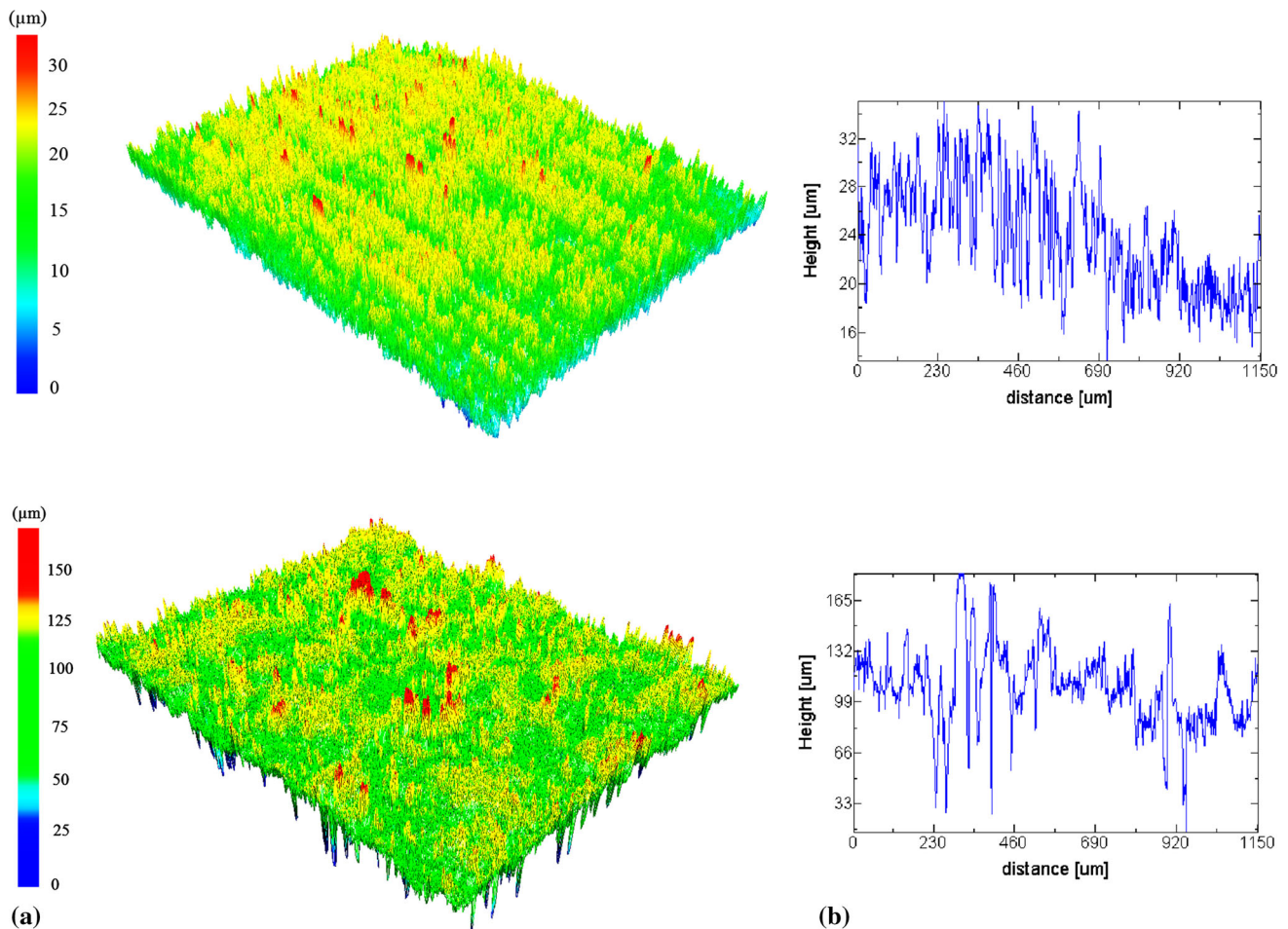


Fig. 8 (a) 3-D representation of the surface topology and (b) cross-sectional profile of the front surface of the smooth (top) and rough (grit-blasted) (bottom) aluminum 6061-T6 substrates

Table 2 Average roughness, skewness, and kurtosis of the smooth and the rough (grit-blasted) aluminum 6061-T6 substrates

Aluminum 6061-T6 substrate	R_{ave} , μm	R_{sk}	R_{ku}
Smooth	3.33	0.39	2.51
Rough (grit-blasted)	13.93	- 0.59	5.28

roughness parameters for both the smooth and rough aluminum substrates that were used in this study.

According to the results presented in Fig. 8 and Table 2, grit-blasting significantly increased the average roughness of the substrate and created steep asperities on the surface of the substrate, as evidenced by the increase in R_{ku} . The negative value of skewness of the substrate after grit-blasting indicates that the grit-blasted surface consisted of deep valleys with smooth plateaus. There were also a greater number of asperities on the rough surface, and their heights were larger than those on the smooth surface. This can be related to the physical structure of the garnet sand

particles. As shown in Fig. 2, garnet sand consisted of particles with smooth and rounded edges. The rounded shape of the particles highly tends to generate surfaces with deep valleys, rather than pointed and sharp peaks after deposition on the substrate. With knowledge of the surface topology of the substrates, a qualitative comparison of the gas-substrate heat transfer coefficient between the smooth and rough substrate can be made.

It is likely that the increased roughness of the substrate would result in an increase in heat transfer coefficient between the impinging air jet and the substrate. Increasing the roughness of the substrate would likely result in higher magnitudes of the velocity fluctuations within the boundary layer of the impinging, spreading jet over the substrate because of tripping of the boundary layer flow that may occur. It was experimentally reported that roughness with heights of 15 to 25 percent of the boundary layer thickness increased both the longitudinal and vertical components of the velocity fluctuations (Ref 26). As a result, the turbulence intensity of the flow, T_u , would increase, since it is

defined as the ratio of the root-mean-square of the fluctuating velocity component and the mean velocity of the flow. The ratio is expressed as (Ref 26)

$$T_u = \frac{\overline{(u')^2}}{\bar{u}_m}^{1/2} \tag{Eq 18}$$

Higher values of turbulence intensity and greater velocity fluctuation will produce higher shear stress in the turbulent flow over the substrate. Increased shear stress induced by the fluid on the substrate will be due to the increased velocity gradients, and momentum transfer by eddies within the turbulent boundary layer. A fundamental study by Reynolds (Ref 27) has shown that the heat transfer between the flow and the substrate is directly proportional to the fluid shear stress on the substrate. The aforementioned theory, known generally as the Reynolds analogy between shear stress and heat transfer, is expressed as (Ref 21)

$$\frac{\bar{h}}{\rho \bar{u}_m C_p} = \frac{C_f}{2} \tag{Eq 19}$$

where \bar{h} is the average heat transfer coefficient. In Eq 19, C_f is the skin friction coefficient and it is defined as (Ref 21)

$$C_f = \frac{\tau_w}{0.5 \rho \bar{u}_m^2} \tag{Eq 20}$$

The Reynolds analogy is a simplified model that may be used as a first approximation of the heat transfer coefficient of and heat transfer from turbulent boundary layer flows over flat plates. The analogy is based on the assumption that the Prandtl number is unity. For air, the Prandtl number is approximately 0.71, which is close to unity. With the exception of the stagnation point where the air jet impacts the surface, it can reasonably be assumed that the jet that spreads radially over the surface does so as flow over a flat plate surface. Since increasing the roughness of the substrate would produce higher skin friction coefficient, resulting in an increase in heat transfer coefficient, this would in turn increase heat exchange between the air jet and the substrate. As a result of the increased heat exchange between the under-expanding air jet and the substrate, higher surface temperatures of the roughened substrate are expected. In order to confirm the aforementioned hypothesis, the steady-state surface temperatures of both smooth and rough substrates were measured by using an infrared camera. Since the measurement of the infrared camera was dependent on the emissivity of the surface, the emissivity of the roughened aluminum substrate was first obtained experimentally.

Emissivity, ϵ , is the ratio of the intensity of emitted radiation from a surface to that emitted from a black body

at a specific temperature. The radiation emitted from the real surface and the black body depends on both wavelength and the surface temperature (Ref 28). The maximum wavelength emitted from the surface directly depends on the surface temperature, according to Wien’s displacement law that $\lambda_{max} T = 2898 \mu\text{m K}$ (Ref 29). Therefore, the emissivity of the surface depends on the surface temperature. In order to measure the surface temperature of the grit-blasted substrate by using the infrared camera, the temperature-dependent emissivity of the substrate had to be evaluated first. Figure 9 shows the emissivity of the grit-blasted aluminum substrate as a function of the surface temperature. The temperature range in Fig. 9 was selected to be in accordance with the range of surface temperatures that was collected for the smooth substrate. It was found that the emissivity of the roughened aluminum substrate at temperatures higher than 100 °C approached 0.32, as shown in Fig. 9. Therefore, this estimated emissivity was used to estimate the steady-state surface temperature of the roughened substrate.

The steady-state surface temperatures of both the smooth and rough substrates were measured by using the infrared camera. The cold spray unit was utilized to cause the impingement of the supersonic air jet at a total pressure of 660 kPa and a total temperature of 300 °C on substrates with thickness of 2.5 mm. Figure 10 shows the comparison of the radial variation of the non-dimensional steady-state surface temperature of the rough substrate with that of the smooth substrate under the same cold spray process conditions. The steady-state surface temperature was non-dimensionalized as

$$\theta_{ss} = \frac{T_{ss} - T_{\infty}}{T_a - T_{\infty}} \tag{Eq 21}$$

As observed in Fig. 10, the steady-state surface temperature of the rough substrate was higher than that of the

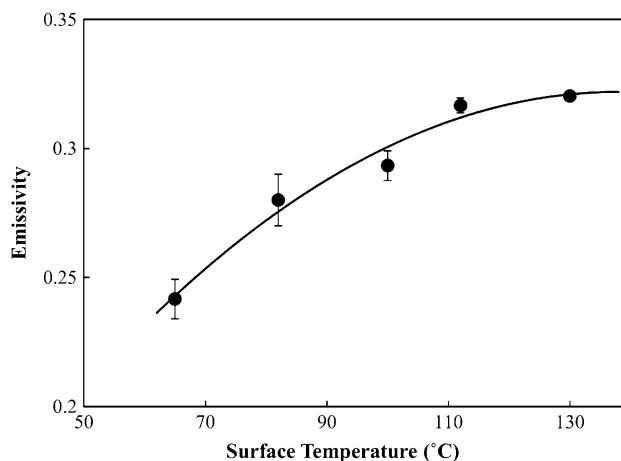


Fig. 9 Emissivity of the grit-blasted Al 6061-T6 substrate at different surface temperatures

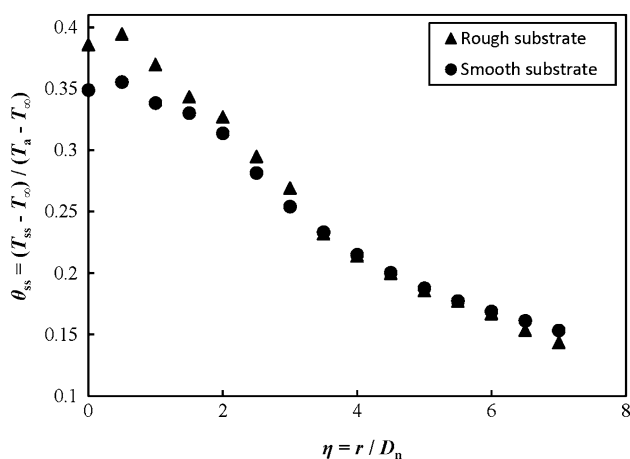


Fig. 10 Comparison of the radial variation of the non-dimensional steady-state surface temperature of the rough and smooth substrates under cold spray air jet impingement

smooth substrate in the vicinity of the stagnation point of the impinging air jet. The measurements of the steady-state surface temperature of the rough substrate were taken by assuming that the emissivity of the rough surface was close to 0.32. This assumption was made since the surface temperature, especially that at the vicinity of the stagnation point of the impinging air jet, was above 100 °C. The result in Fig. 10 confirmed that the surface roughness would increase the surface temperature as a result of an increase in the heat transfer coefficient and heat transfer from the air jet to the substrate. In addition to the influence of the heat transfer coefficient on the increased surface temperature, the increased surface area of the rough substrate due to the asperities on the surface may have increased the heat transfer rate from the air to the surface, thus increasing the surface temperature. By comparing the cross-sectional profile of the smooth and rough substrates shown in Fig. 8, it is observed that there are more asperities on the rough surface and the height of those asperities are greater than those that are observed on the smooth surface. The asperities may act as fins, which extend and increase the surface area of the grit-blasted substrate, increasing the heat transfer rate. The increased heat transfer rate due to the increased surface area may be explained by way of Newton’s Law of Cooling (Ref 29), which states that

$$\dot{Q} = hA_s\Delta T, \tag{Eq 22}$$

where A_s is the surface area through which the heat exchange occurs. The equation confirms that as the surface area increases, the heat transfer rate (\dot{Q}) from the air jet to the substrate increases. Also, according to Table 2, the high values of kurtosis produced steep asperities on the rough surface, enhancing the performance of the extended surfaces or fins. The asperity fins, by increasing the heat

transfer rate, produced higher surface temperatures on the rough substrate.

Observations from Fig. 10 also suggest that the steady-state surface temperature of the rough substrate did not differ from that of the smooth substrate at distances that were farther downstream from the stagnation point. It is likely that the surface temperature measurements at those regions might be significantly affected by the inevitable errors in the estimates of emissivity of the substrate. Since the temperature of the surface decreased as the distance from the stagnation point increased, the emissivity of the substrate likely decreased as well. Since the infrared camera used a fixed value of emissivity as an input, in this case it was set at 0.32, there was likely some error in the surface temperature measurements taken at points that were farther downstream from the stagnation point. Having taken into account the possible errors in the temperature measurement in those regions, it was also possible that due to the higher heat transfer rate between the under-expanding air jet and the rough substrate in the vicinity of the stagnation point, the air that reached the outer regions of the substrate became cooler, resulting in lower temperature rise in comparison with flow over the smooth substrate.

Effect of Substrate Thickness on Heat Transfer Coefficient and Surface Temperature Profile

The surface temperature profile of the substrate under an impinging air jet may be affected by the thickness of the substrate. It is, however, expected that the heat transfer coefficient of the impinging air jet on the substrate will be independent of the thickness of the substrate since the heat transfer coefficient mainly depends on geometry of the surface that is in contact with the fluid, the fluid properties, the flow regime (that is, laminar or turbulent flow), and in some cases, the temperature difference between the fluid and the surface (Ref 28). Therefore, the effect of the substrate thickness on the heat transfer coefficient of the impinging air jet and the surface temperature of the substrate was investigated. The cold spray unit was utilized to cause the impingement of the compressed air jet on the substrate at a total temperature of 300 °C and at a total pressure of 660 kPa. The heat transfer coefficient that was estimated for a substrate with thickness of 1.5 mm was substituted into Eq 7. The non-dimensional surface temperature of the substrate was calculated at a Fourier number of 81 and for substrate thicknesses of 2.5 and 6.5 mm. Figure 11 shows a comparison of the estimated and experimentally measured non-dimensional surface temperature for the different thicknesses. Although the heat transfer coefficient, which was used in the calculations, was measured at $\delta = 1.5$ mm, the results of the semi-empirical analytical model that pertain to the thicker

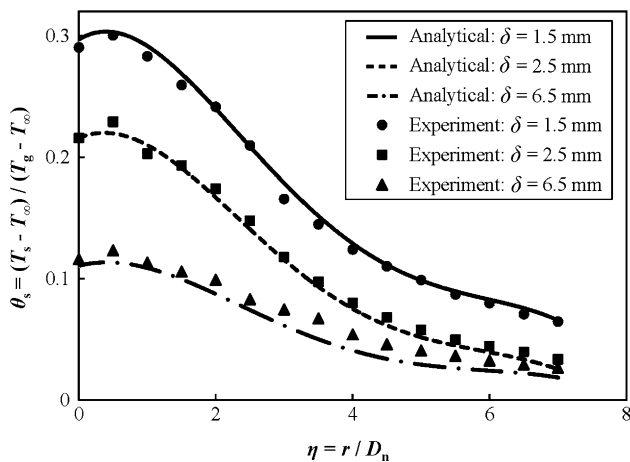


Fig. 11 Comparison of predicted and experimentally measured non-dimensional surface temperature variation of the substrate at different substrate thicknesses

substrates was in close agreement with the experimental results, confirming that the heat transfer coefficient of an impinging air jet upon the substrate was independent of the thickness of the substrate. It was also observed that the surface temperature of the substrate decreased as the radial distance from the stagnation point of the impinging air jet increased, and as the thickness of the substrate increased. A similar observation was reported by McDonald et al. (Ref 15). Due to the increase in the thickness of the substrate, the volume of the substrate increased; thus, a higher quantity of thermal energy was conducted through the substrate. Therefore, the surface temperature of the thicker substrate was lower than that of the substrate with lower thickness (Ref 15).

Conclusion

In this study, the effect of substrate and cold spray process parameters on the heat transfer coefficient between the substrate and the impinging air jet was investigated. Surface temperature profiles that occurred during the cold spray jet impingement were also developed. A low-pressure cold-gas dynamic spraying unit was used to produce a compressed supersonic air jet that impinged on a flat substrate. A detailed mathematical model was developed and coupled with experimental data to estimate the heat transfer coefficient and the surface temperature of the substrate. The effect of the total pressure and temperature of the air jet, as the process parameters, on the heat transfer coefficient was studied. It was found that increasing the total pressure of the air would increase the Nusslet number of the impinging air jet at all locations downstream of the stagnation point. It was further found that increasing the total temperature of the air jet did not affect the Nusselt

number; however, it slightly increased the heat transfer coefficient of the impinging air jet on the substrate.

The effect of the roughness and thickness of the substrate, as the substrate parameters, on the surface temperature of the substrate and the heat transfer coefficient was studied. The heat transfer coefficient of the impinging air jet on a roughened (grit-blasted) substrate increased, compared to that on a smooth substrate. It was further found that the heat transfer coefficient is independent of the thickness of the substrate. Moreover, it was shown that as the thickness of the substrate increased, the surface temperature decreased at all points downstream of the stagnation point. The heat transfer coefficient that was estimated for a substrate with thickness of 1.5 mm was substituted into the semi-empirical analytical model to determine the surface temperature of the substrate at different thicknesses. The results were compared to the experimental data and there was good agreement between the predicted and experimentally measured surface temperatures.

Acknowledgments The authors also wish to acknowledge the financial support of the Natural Science and Engineering Research Council of Canada (NSERC), the Canadian Foundation for Innovation (CFI), and the Government of Alberta. The authors of this study gratefully thank Dr. David Nobes for providing the infrared camera that was used.

References

1. V.F. Kosarev, S.V. Klinkov, A.P. Alkhimov, and A.N. Papyrin, On Some Aspects of Gas Dynamics of the Cold Spray Process, *J. Therm. Spray Technol.*, 2003, **12**(2), p 265-281
2. M. Faizan Ur Rab, S. Zahiri, S. Masood, M. Jahedi, and R. Nagarajah, Development of 3D Multicomponent Model for Cold Spray Process Using Nitrogen and Air, *Coatings*, 2015, **5**, p 688-708
3. M.D. Limaye, R.P. Vedula, and S.V. Prabhu, Local Heat Transfer Distribution on a Flat Plate Impinged by a Compressible Round Air Jet, *Int. J. Therm. Sci.*, 2010, **49**, p 2157-2168
4. S. Yin, X. Wang, W. Li, and X. Guo, Examination on Substrate Preheating Process in Cold Gas Dynamic Spraying, *J. Therm. Spray Technol.*, 2011, **20**(4), p 852-859
5. Y. Watanabe, C. Yoshida, K. Atsumi, M. Yamada, and M. Fukumoto, Influence of Substrate Temperature on Adhesion Strength of Cold-Sprayed Coatings, *J. Therm. Spray Technol.*, 2015, **24**(1-2), p 86-91
6. E. Irissou, J.G. Legoux, A. Ryabinin, B. Jodoin, and C. Moreau, Review on Cold Spray Process and Technology: Part I—Intellectual Property, *J. Therm. Spray Technol.*, 2008, **17**, p 495-516
7. T. Schmidt, H. Assadi, F. Gartner, H. Richter, T. Stoltenhoff, H. Kreye, and T. Klassen, From Particle Acceleration to Impact and Bonding in Cold Spraying, *J. Therm. Spray Technol.*, 2009, **18**(5-6), p 794-808
8. J.G. Legoux, E. Irissou, and C. Moreau, Effect of Substrate Temperature on the Formation Mechanism of Cold-sprayed Aluminum, Zinc and Tin Coating, *J. Therm. Spray Technol.*, 2007, **16**(5-6), p 619-626

9. M. Fukumoto, H. Wada, K. Tanabe, M. Yamada, E. Yamaguchi, A. Niwa, M. Sugimoto, and M. Izawa, Effect of Substrate Temperature on Deposition Behavior of Copper Particles on Substrate Surface in the Cold Spray Process, *J. Therm. Spray Technol.*, 2007, **16**(5-6), p 643-650
10. T. Stoltenhoff, H. Kreye, and H. Richter, An Analysis of Cold Spray Process and Its Coating, *J. Therm. Spray Technol.*, 2002, **11**, p 542-550
11. P. King, G. Bae, S. Zahiri, M. Jahedi, and C. Lee, An Experimental and Finite Element Study of Cold Spray Copper Impact Onto Two Aluminum Substrates, *J. Therm. Spray Technol.*, 2010, **19**, p 620-634
12. W. Chakroun, A. Abdel-Rahman, and S. Al-Fahed, Heat Transfer Augmentation for Air Jet Impinged on a Rough Surface, *Appl. Therm. Eng.*, 1998, **18**, p 1225-1241
13. A. Beitelmal and M. Saad, Effects of Surface Roughness on the Average Heat Transfer of an Impinging Air Jet, *Int. Commun. Heat Mass Transf.*, 2000, **27**, p 1-12
14. M.M. Cobberteau and M.M. Rahman, Numerical Analysis of Steady State Heat Transfer for Jet Impingement on Patterned Surfaces, *Appl. Therm. Eng.*, 2016, **103**, p 481-490
15. A. McDonald, A. Ryabinin, E. Irissou, and J.G. Legoux, Gas-Substrate Heat Exchange during Cold-Gas Dynamic Spraying, *J. Therm. Spray Technol.*, 2012, **22**(2-3), p 391-397
16. H. Ashrafizadeh, P. Mertiny, and A. McDonald, Evaluation of the Effect of Temperature on Mechanical Properties and Wear Resistance of Polyurethane Elastomers, *Wear*, 2016, **368**(9), p 26-38
17. A. Mahdavi and A. McDonald, *Effect of Substrate Roughness and Thickness on the Gas-Substrate Convective Heat Transfer during Cold Spraying*, *Thermal Spray 2017: Proceedings of the International Thermal Spray Conference*, June 7-9, 2017 (Düsseldorf, Germany), ASM International, 2017, p 1-6.
18. A. Mahdavi and A. McDonald, *Analytical Evaluation of Temperature Distribution within the Substrate under an Impinging Cold Spray Hot Air Jet*, *Thermal Spray 2016: Proceedings of the International Thermal Spray Conference*, May 10-12, 2016 (Shanghai, People's Republic of China), ASM International, 2016, p 1-5.
19. Y.A. Çengel and J.M. Cimbala, *Fluid Mechanics: Fundamentals and Applications*, 3rd ed., McGraw-Hill Inc, New York, 2013
20. Y.A. Çengel and M.A. Boles, *Thermodynamics: An Engineering Approach*, 8th ed., The McGraw-Hill Companies Inc, New York, 2014
21. A. Shapiro, *The Dynamics and Thermodynamics of Compressible Fluid Flow*, Vol II, The Ronald Press Company, New York, 1954
22. U. Prisco, Size-dependent Distribution of Particle Velocity and Temperature at Impact in the Cold-gas Dynamic-Spray Process, *J. Mater. Process. Technol.*, 2015, **216**, p 302-314
23. C.W. Ziemian, M.M. Sharma, B.D. Bouffard, T. Nissley, and T.J. Eden, Effect of Substrate Surface Roughening and Cold Spray Coating on the Fatigue Life of AA2024 Specimens, *Mater. Des.*, 2014, **54**, p 212-221
24. A. McDonald, M. Lamontagne, S. Chandra, and C. Moreau, Photographing Impact of Plasma-Sprayed Particles on Metal Substrate, *J. Therm. Spray Technol.*, 2006, **15**(4), p 708-716
25. P. Chauvy, C. Madore, and D. Landolt, Variable Length Scale Analysis of Surface Topography: Characterization of Titanium Surfaces for Biomedical Applications, *Surf. Coat. Technol.*, 1998, **110**, p 48-56
26. L. Lyles, L.A. Disrud, and R.K. Krauss, Turbulence Intensity as Influenced by Surface Roughness and Mean Velocity in a Wind-tunnel Boundary Layer, *Trans. ASAE*, 1971, **14**, p 285-289
27. O. Reynolds, On the Extent and Action of the Heating Surface of Steam Boilers, *Proc. Lit. Philos. Soc., Manchester*, 1874, **4**, p 7-12
28. C. Wen and I. Mudawar, Emissivity Characteristics of Roughened Aluminum Alloy Surfaces and Assessment of Multispectral Radiation Thermometry (MRT) Emissivity Models, *Int. J. Heat. Mass. Transf.*, 2004, **47**, p 3591-3605
29. L. Jiji, *Heat Convection*, 2nd ed., Springer, New York, 2009